

Impact of QCD jets and heavy-quark production in cosmic-ray proton atmospheric showers up to 10^{20} eV

David d'Enterria,¹ Tanguy Pierog,² and Guanhao Sun^{1,3,4}

¹CERN, EP Department, 1211 Geneva, Switzerland

²Karlsruhe Institute of Technology (KIT), IKP, Postfach 3640, 76021 Karlsruhe, Germany

³Hong Kong Univ. of Science and Technology, HKUST, Hong Kong, China

⁴Center for Theoretical Physics and Dept. of Physics, Columbia Univ., New York, NY 10027, USA

The PYTHIA 6 Monte Carlo (MC) event generator, commonly used in collider physics, is interfaced for the first time with a fast transport simulation of a hydrogen atmosphere, with the same density as air, in order to study the properties of extended atmospheric showers (EAS) produced by cosmic ray protons with energies $E_{\text{CR}} \approx 10^{14}$ – 10^{20} eV. At variance with the hadronic MC generators (EPOS-LHC, QGSJET, and SIBYLL) commonly used in cosmic-rays physics, PYTHIA includes the generation of harder hadronic jets and heavy (charm and bottom) quarks, thereby producing higher transverse momentum final particles, that could explain several anomalies observed in the data. The electromagnetic, hadronic, and muonic properties of EAS generated with various settings of PYTHIA 6, tuned to proton-proton data measured at the LHC, are compared to those from EPOS-LHC, QGSJET 01, QGSJET-II-04, and SIBYLL 2.1. Despite their different underlying parton dynamics, the characteristics of the EAS generated with PYTHIA 6 are in between those predicted by the rest of MC generators. The only exceptions are the muonic components at large transverse distances from the shower axis, where PYTHIA predicts more activity than the rest of the models. Heavy-quark production, as implemented in this study for a hydrogen atmosphere, does not seem to play a key role in the EAS muon properties, pointing to nuclear effects as responsible of the muon anomalies observed in the air-shower data.

I. INTRODUCTION

Ultrahigh-energy cosmic rays (UHECR) with energies up to $E_{\text{CR}} \approx 10^{20}$ eV are the most energetic particles known in the universe. Their exact nature and origin, protons or heavier ions accelerated in various extreme extragalactic environments, remain still open questions today (see e.g., [1, 2] for recent reviews). The flux of UHECR impinging on earth is very scarce (less than 1 particle per km^2 per century at the highest energies), and their detection is only possible through the huge extensive air showers (EAS) of secondary particles that they produce in electromagnetic and hadronic interactions with the nitrogen and oxygen nuclei in the atmosphere. These showers include an electromagnetic (e.m.) component consisting of electrons, positrons, and photons (mostly coming from the $\pi^0 \rightarrow \gamma\gamma$ decays of the produced neutral pions); a hadronic component mostly consisting of protons, neutrons, and charged pions and kaons; as well as muonic and neutrino components (mostly issuing from the hadronic shower, via decays of charged pions and kaons). As the cascade develops in the atmosphere, the number of particles in the shower increases until the energy of the secondary particles is degraded to the level where ionization losses dominate. At this point –as the particles only lose energy, are absorbed, or decay– the density of particles starts to decline. In each generation about 20% of the energy is transferred to the electromagnetic cascade that, ultimately, dissipates roughly 90% of the primary particle's energy through ionization of the atmosphere atoms. Dedicated observatories exist, such as the Pierre Auger Observatory [3] and the Telescope Array (TA) [4], that determine the energy and mass of the incoming UHECR in arrays of detectors by (i) sampling the fraction of the EAS particles that reach ground and/or, in moonless nights, by measuring (ii) the fluorescence photons that are produced by nitrogen molecules excited by the particle shower.

Usually the distance along the EAS axis is measured as a column density X (longitudinal shower profile, measured in g cm^{-2}), indicating the amount of air traversed downstream from the top of the atmosphere in the direction of the shower propagation. For reference, the total vertical column density at sea-level is about $1\,000 \text{ g cm}^{-2}$, and the total column density for a shower traversing the atmosphere at zenith angle of $\theta = 60^\circ$ is twice larger. A *vertically-incident* 10^{20} eV proton produces about 10^{11} secondaries at sea-level with energies above 90 keV in the annular region extending from 8 m to 8 km off the shower axis. Of these, 90% are γ 's, 9% e^\pm , and 1% μ^\pm plus charged hadrons. The mean energy of e.m. particles is around 10 MeV and they transport 85% of the total energy at ground level. These numbers change dramatically for the case of very inclined showers. For a primary zenith angle, $\theta > 60^\circ$, the electromagnetic component becomes attenuated exponentially with atmospheric depth, being almost completely absorbed at ground. For this reason, inclined showers with $\theta \approx 60^\circ$ are particularly useful to probe the hadronic and muonic properties of the cascades, and will be studied in detail in this work.

The determination of the original UHECR energy and mass is based on a detailed comparison of the EAS

properties to the predictions of Monte Carlo (MC) models of the hadronic and electromagnetic development of the particle shower. Key EAS observables are the average depth of the shower maximum $\langle X_{\max} \rangle$ and the RMS width of its fluctuations $\sigma_{X_{\max}}$, the number and total energy of electrons (N_e, E_e) and muons (N_μ, E_μ) on ground for various shower zenith angle (θ) inclinations. The primary mass composition and energy of UHECR is thereby extracted by comparing the experimental measurements to the results of full MC simulations of the EAS development in the atmosphere for different incoming species (protons, He, N, and Fe ions, mostly) at various initial candidate energies. This is commonly done with transport programs such as CORSIKA [5] interfaced to a set of hadronic interaction models such as EPOS [6], EPOS-LHC [7], QGSJET 01 [8, 9], QGSJET-II-04 [10], or SIBYLL 2.1 [11] for the hadronic interactions, plus EGS4 [12] for the e.m. cascade evolution. All these hadronic interaction models describe the inclusive production of particles in high-energy proton and nucleus collisions based on basic quantum field-theory principles –such as unitarity and analyticity of scattering amplitudes– as implemented in the framework of Gribov’s Reggeon Field Theory (RFT) [13], extended to take into account perturbative quantum chromodynamics (pQCD) scatterings in (multiple) harder parton-parton collisions via “cut (hard) Pomerons” (understood diagrammatically as a ladder of gluons). With model parameters tuned to reproduce the existing accelerator and collider results* [14], all those MC generators are able to describe the overall EAS properties, although some “anomalies” persist in the UHECR data that cannot be easily accommodated. On the one hand, the $\langle X_{\max} \rangle$ and $\sigma_{X_{\max}}$ dependence on E_{CR} indicates a change of cosmic ray composition from proton-dominated to a proton-iron mix above $E_{\text{CR}} \approx 10^{19}$ eV [15, 16], but quantitative differences in $\langle X_{\max} \rangle$ exist, of up to 40 g cm^{-2} among model predictions, that are not-fully understood, even though independently each MC event generator reproduces the LHC data [17–19]. On the other hand, in the same range of E_{CR} energies, recent Auger measurements indicate about 30–60% more muons on ground than expected by any of the MC models [20, 21]. A similar result was observed longer ago by the HiRes-MIA hybrid array, with a higher density of muons at 600 m from the shower’s trajectory than expected from the (then current) hadronic interaction event generators [22]. Those findings suggest that the best models of hadronic interactions are missing some physics ingredient. Either they do not account for processes that produce harder muons, such as from e.g., hard jets or heavy-quark (in particular charm [23]) decays, and/or they do not feed enough energy into the hadronic component of the EAS (such as e.g., through an increased production of baryon-antibaryon pairs [24]). More speculative explanations have been put forward based on changes in the physics of strong interactions at energies beyond those tested at the LHC [25, 26].

The main purpose of this work is to test whether the aforementioned UHECR data–model differences can be explained as due to missing perturbative processes in the RFT-based approaches. For this purpose, hadronic collisions are generated with the standard MC event generator used in particle physics, PYTHIA 6 [27] based on a purely pQCD framework that includes the production of rarer processes such as (multiple) high transverse momentum jets and heavy-quarks (charm and bottom). Despite its success in reproducing a large amount of experimental proton-(anti)proton collider data through tuned settings of its model parameters [28], PYTHIA has never been used to study cosmic rays interactions as it cannot deal (so far) with the proton-nucleus or nucleus-nucleus interactions encountered in UHECR collisions with air nuclei. In order to overcome this limitation, we construct first a hydrogen atmosphere where the only target “nuclei” present are protons, with a density matching that of air, using the fast CONEX transport simulation [29]. Second, we interface PYTHIA 6, with various settings of its MC parameters, as well as the rest of RFT-based models, with CONEX in order to generate the corresponding extended “air” showers from incoming proton cosmic rays with energies $E_{\text{CR}} \approx 10^{14}$ – 10^{20} eV, and compare the properties of the resulting electromagnetic, hadronic, and muonic EAS components.

II. THEORETICAL SETUP

A. CONEX air-shower simulation

For primary cosmic rays of energies above $E_{\text{CR}} \approx 10^{18}$ eV, full simulations of their EAS development performed with the CORSIKA program [5] are time-consuming, and a systematic study of the shower properties for many variations of the underlying hadronic interaction models settings is prohibitive in practical terms. A viable alternative consists in using a hybrid air-shower scheme, such as that implemented in CONEX [29], effectively combining two main stages: an explicit MC simulation of particle cascading at energies above some chosen threshold E_{thr} (typically a factor of 100 smaller than the energy E_{CR} of the incoming primary particle),

* The nominal LHC proton-proton center-of-mass (c.m.) energy, $\sqrt{s} = 14 \text{ TeV}$, corresponds to UHECR of $E_{\text{CR}} \approx 10^{17}$ eV colliding with air nuclei at rest.

plus a numerical solution of the hadronic-electromagnetic cascade equations for sub-cascades at smaller energies. For the first part of the EAS development, the simulation of all particle interactions and decays is taken care of by the chosen interfaced high-energy hadronic interaction model (here PYTHIA 6, EPOS-LHC, QGSJET-II-04, QGSJET 01, and SIBYLL 2.1), and the characteristics of all produced particles (type, energy, and slant depth position) below E_{thr} are written into corresponding stacks or “source terms”. Such sources provide the initial conditions for the subsequent fast numerical solution of the equations describing the second part of the cascade, calculated only along the direction of the shower axis. The final results are discretized energy spectra of all particles of different types at various depth shower positions. In the first MC cascade step, CONEX follows the propagation, interaction and decay (where applicable) of (anti)nucleons and (anti)hyperons, charged and neutral pions/kaons, whereas all other types of hadrons produced in interactions (including D and B heavy-quark hadrons in the case of PYTHIA) are assumed to decay immediately. The MC e.m. cascade is realized with the EGS4 code, complemented with the Landau-Pomeranchuk-Migdal effect for ultra-high energy e^\pm and γ . In the second analytical step, the system of coupled e.m. cascade equations is based on the same interaction processes implemented in the MC (Bethe-Heitler for bremsstrahlung and pair production, Klein-Nishina for the Compton process, Möller and Bhabha processes, as well as e^+e^- annihilation). In order to generate the lateral distribution of the EAS at ground, low energy particles can be sampled from the energy distribution of particles along the shower axis produced by the cascade equations following the SENECA model approach [30]. Typically, hadrons below 300 GeV, muons at all energies and e.m. particles with less than 10 GeV are then tracked again in the MC cascade, where Coulomb scattering and transverse momentum of the particles can be taken into account. Spatial and temporal distribution of particles are then similar to what can be obtained from a full MC cascade such as CORSIKA [30, 31]. In this work, the CONEX programme is initialized with a modified model of the earth atmosphere, changing N and O atomic nuclei by hydrogen alone with a density matching that of air, and interfaced with PYTHIA 6 as well as with the other four hadronic MC models. With such a setup we generate multiple “fixed-target” proton-proton (pp) collisions over the range of energies $E_{\text{CR}} \approx 10^{14} - 10^{20}$ eV. Hereafter, the results shown for “sea-level” will refer to a ground at the sea level of 0 m ($\sim 1\,000$ g cm $^{-2}$ vertical depth or $\sim 2\,000$ g cm $^{-2}$ slant depth for shower with a zenith angle θ of 60°).

B. PYTHIA 6 Monte Carlo settings

The basic ingredients of PYTHIA 6.428 are leading-order pQCD $2 \rightarrow 2$ matrix elements, complemented with initial- and final-state parton radiation (ISR and FSR), convolved with parton distribution functions (PDFs) for the initial state, and the Lund string model [32] to describe the final parton hadronization. The infrared $1/p_T^4$ divergence of the hard (multi)parton cross section, when the transverse momentum of the minijet $p_T \rightarrow 0$, is regularized by a cutoff Q_0 , such that $1/p_T^4 \rightarrow 1/(p_T^2 + Q_0^2)^2$, that depends on a power ϵ of the pp c.m. energy: $Q_0^2(s) = Q_0^2(s_0) \cdot (s/s_0)^\epsilon$, where $Q_0(s_0) \approx 2.5$ GeV is a reference value at a given c.m. energy $\sqrt{s_0} \approx 7$ TeV. The values of the Q_0 and ϵ parameters impact the total hadron multiplicity in a given pp collision: a *higher* scaling power of the infrared cut-off implies a *slower* increase of the overall hadronic activity. Other non-perturbative ingredients of PYTHIA include a Regge-based modeling of diffractive processes [33], plus a model for the underlying-event issuing from multi-parton interactions (MPI), soft scatterings, and beam-remnants [34]. The MPI are treated perturbatively based on an impact-parameter-dependent transverse overlap of the colliding protons, described by a Gaussian profile in all the settings considered here.

In this work, seven different sets of model parameters (tunings) of PYTHIA 6.428 are considered via the PYTUNES switch for the description of semihard (ISR and FSR showering) and non-perturbative (hadronization) dynamics. The default settings are those of the central “Perugia” (350) tune fitted to underlying event (UE), minimum bias (MB), and Drell-Yan measurements from 2011 pp collisions at the LHC [28], using the CTEQ5L PDFs [35]. The production and decay of secondary charm and bottom hadrons is handled directly by PYTHIA 6, namely we do not consider their possible direct interaction with the “target” partons of atmospheric protons. We also run the 350 tune with heavy-quark production explicitly switched-off[†] in order to estimate the impact of charm and bottom production on the shower properties. In addition, the following five other tune variations, based on 2012 LHC data using the CTEQ6L parton densities [36], with slightly increased strangeness ($s\bar{s}$, η , η') production and softer baryon spectra compared to the 350 tune, are used:

- (i) tune 371 with high ISR and FSR obtained evaluating the QCD coupling at a scale $\alpha_s(p_T/2)$,

[†] Technically, this is done by setting 3 flavours only (u, d, s) in ISR (MSTP (58) = 3) and FSR (MSTJ (45) = 3), and by switching off gluon splittings into charm and bottom: IDCC=MDCY (21, 2) -1+4, IDCB=MDCY (21, 2) -1+5, MDME (IDCC, 1) = 0, MDME (IDCB, 1) = 0.

- (ii) tune 372 with low ISR and FSR obtained using $\alpha_s(2p_T)$,
- (iii) tune 380, using only gluon-gluon processes at low- p_T , without valence-quark scattering ($\text{PARP}(87)=0$),
- (iv) tune 381, with lower values of the Q_0 and ϵ parameters leading to a higher amount of UE activity,
- (v) tune 382, with higher values of the Q_0 and ϵ parameters leading to a lower amount of UE activity.

Table I provides a summary of the seven PYTHIA 6 MC tune settings considered in this work. We note also that the overall properties of particle production of the chosen set of PYTHIA 6 tunes are very similar to those obtained with the latest tunes of the PYTHIA 8 version of the code [37], as discussed in Ref. [38].

PYTHIA 6.428 Perugia tune PYTUNES number (main features)	PDF	Q_0 cutoff at $\sqrt{s_0} = 7$ TeV	Q_0 scaling power ϵ	ISR/FSR scale $\alpha_s(k \cdot p_T)$	Hadronization
350 (central tune 2011)	CTEQ5L1	2.93 GeV	0.265	$k = 1$	$s\bar{s}, \eta, \eta'$ suppr. = 95,63,12%
350, noHQ (central 2011; no c-,b-quarks)	CTEQ5L1	2.93 GeV	0.265	$k = 1$	$s\bar{s}, \eta, \eta'$ suppr. = 95,63,12%
371 (var. 2012, high rad.)	CTEQ6L1	2.72 GeV	0.25	$k = 1/2$	$s\bar{s}, \eta, \eta'$ suppr. = 92,70,13.5%; softer baryons
372 (var. 2012, low rad.)	CTEQ6L1	2.60 GeV	0.23	$k = 2$	$s\bar{s}, \eta, \eta'$ suppr. = 92,70,13.5%; softer baryons
380 (var. 2012, gg only at low- p_T)	CTEQ6L1	2.65 GeV	0.245	$k = 1$	$s\bar{s}, \eta, \eta'$ suppr. = 92,70,13.5%; softer baryons
381 (var. 2012, higher UE)	CTEQ6L1	2.46 GeV	0.23	$k = 1$	$s\bar{s}, \eta, \eta'$ suppr. = 92,70,13.5%; softer baryons
382 (var. 2012, lower UE)	CTEQ6L1	2.92 GeV	0.26	$k = 1$	$s\bar{s}, \eta, \eta'$ suppr. = 92,70,13.5%; softer baryons

TABLE I: Details of the various ingredients controlling the semi-hard and non-perturbative dynamics in the seven tunes of PYTHIA 6.428 used in this work. See text and [28] for details.

C. RFT-based Monte Carlo event generators

In the standard RFT-based MCs used in cosmic-ray physics (EPOS-LHC, QGSJET-II-04, QGSJET 01, and SIBYLL 2.1), hadronic collisions are generated starting from a construction of the scattering amplitude to determine the total and elastic cross sections with intercept and slope of the Pomeron (\mathbb{P}) Regge trajectory, Pomeron-hadron couplings, etc. fixed from experimental data. Inelastic events are generated “cutting” diagrams involving multiple- \mathbb{P} exchanges based on the so-called Abramovskii-Gribov-Kancheli rules [39]. Cut Pomerons correspond to color flux tubes, treated as strings extended between the colliding partons, that subsequently fragment into hadrons separately following various hadronization models with parameters fitted to reproduce the data. Leading-order pQCD scatterings are modeled, above a scale Q_0 , through multiple “cut hard Pomerons” diagrams. Since fixed-target collisions of protons with 10^{20} eV energies involve gluon interactions with fractional momenta $x \approx p_T / \sqrt{s} \approx 10^{-7}$, three orders-of-magnitude smaller than those currently probed in PDF extractions, the models include various approaches to deal with the onset of non-linear (gluon fusion) effects saturating the growth of the PDFs as $x \rightarrow 0$. The different generators used here differ in various approximations for the collision configurations (e.g., for the number of cut- \mathbb{P} and the energy-momentum partition among them), the treatment of diffractive and perturbative contributions as well as of low- x PDFs, and the details of particle production from string fragmentation. In the QGSJET models, the transverse profile of the proton (the underlying PDF in the impact-parameter direction) is effectively Gaussian, whereas in SIBYLL 2.1 it is taken as the Fourier transform of the proton electric form factor, resulting in an energy-independent exponential fall-off of the transverse PDF. The harder form of the SIBYLL form factor allows a greater retention of energy by the leading particle, and hence less of it available for the ensuing shower. Table II provides a summary of the particle-production properties of the four RFT-based MC event generators considered in this work.

Model (version)	Q_0 hard-soft threshold	Low- x PDF	Hadronization
SIBYLL 2.1	1.0 GeV + exp $\sqrt{\ln s}$	GRV [40]	Lund string fragmentation
QGSJET 01	2.0 GeV	constant	own string fragmentation
QGSJET-II-04	1.6 GeV	non-linear \mathbb{P} corrections + pQCD	own string fragmentation
EPOS-LHC	2.0 GeV	parametrized soft + pQCD	area-law string fragmentation + collective flow

TABLE II: Details of the main ingredients controlling the non-perturbative and semi-hard dynamics present in the RFT-based event generators used in this work.

III. RESULTS

The properties of the extended atmospheric showers predicted by the pQCD- and RFT-based MC generators are studied by running the simulation setup described in the previous Section. For each one of the 14 incoming cosmic-ray proton energies over the range $E_{\text{CR}} \approx 10^{14}, 10^{14.5} \dots 10^{20}, 10^{20.5}$ eV, one thousand air-showers are generated using CONEX interfaced with the seven tunes of PYTHIA 6, as well as with EPOS-LHC, QGSJET-II-04, QGSJET 01, and SIBYLL 2.1 (with their default settings), totaling 154 000 EAS generated and statistically studied. The generic features of the generated showers, given by $\langle X_{\text{max}} \rangle$ and $\sigma_{X_{\text{max}}}$, as well as the properties of their electromagnetic, hadronic, and muonic components are discussed in detail in the following subsections.

A. Generic properties of high-energy pp collisions

The relationship between the key ingredients of hadronic interaction MCs and EAS observables can be extracted using a generalized Heitler type model [41] and has been numerically studied in detail in [42]. The average depth $\langle X_{\text{max}} \rangle$ and fluctuations $\sigma_{X_{\text{max}}}$ of the shower maximum depend chiefly on the characteristics of multiparticle production of the first few generations of hadronic interactions in the shower. The key model ingredients are (i) the *inelastic pp cross section* σ_{inel} (combined with a Glauber model to derive the proton-air cross section [43]), (ii) the *multiplicity* (N_{ch}) of the primary and subsequent very high-energy interactions, which affects how the energy is distributed to secondary particles and corresponding subshowers, and (iii) the *inelasticity* $K = 1 - E_{\text{lead}}/E_{\text{CR}}$ or fraction of the primary particle energy transferred to secondary particles after removing the most energetic “leading” hadron emitted at very forward rapidities. In addition, the *mean transverse momentum* of the particles produced, which is closely related to the peak of the (mini)jet production cross section around the scale Q_0 , is a sensitive quantity of the modeling of the transition from soft to hard scatterings. The level of agreement between the MC predictions for many observables and the LHC data was thoroughly discussed in [14, 38], where it was found that the models overall bracketed the experimental measurements and only small modifications, such as those that led to the PYTHIA 6 tunes of Table I and to the new EPOS-LHC release, were required.

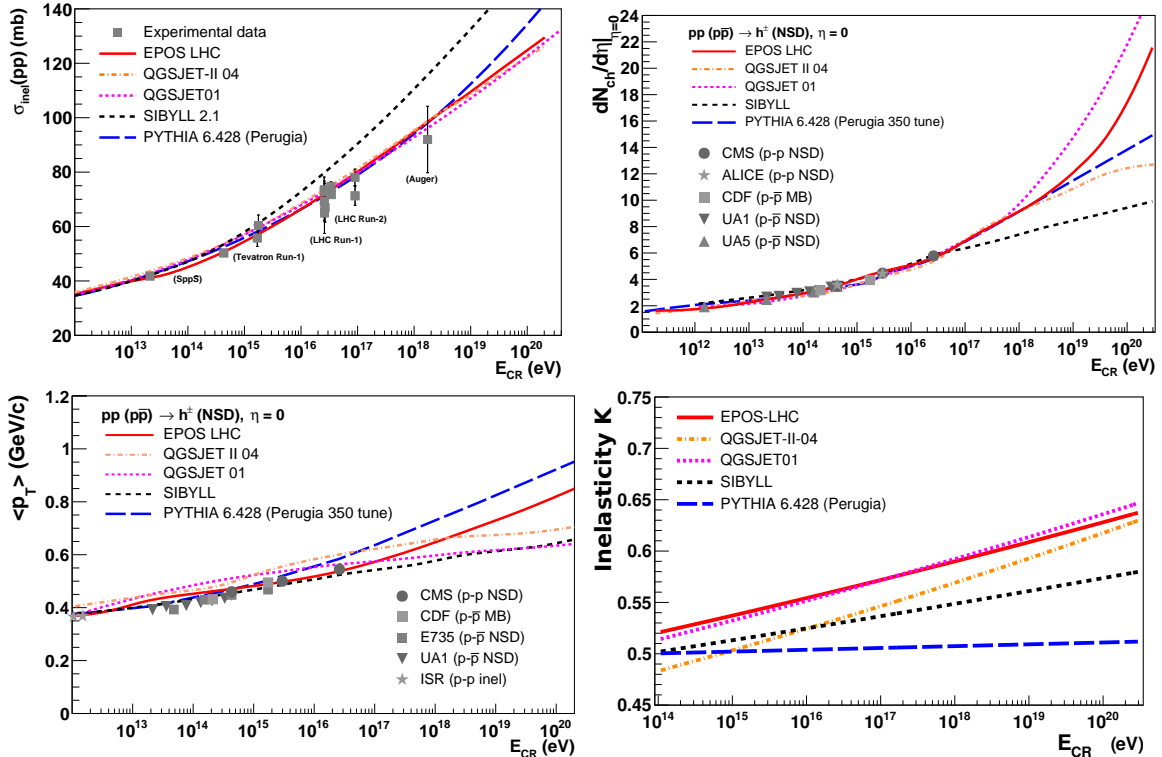


FIG. 1: Cosmic-ray energy dependence of key model ingredients of the MC event generators considered in this work: Inelastic pp cross section (top left), midrapidity charged particle multiplicity density (top right), mean transverse momentum (bottom left), and inelasticity (bottom right). Experimental data points, either from non-single-diffractive (NSD) or “minimum bias” (MB) collisions are from the compilations of Refs. [14, 38].

Figure 1 shows the dependence on incoming cosmic-ray energy of the pp inelastic cross section (top left), charged particle density at midrapidity (top right), mean transverse momentum (bottom left), and pp inelasticity (bottom right). For PYTHIA 6, only the default 350 tune is shown as other tunings, including that inhibiting heavy-flavor production, give identical or very similar results for such inclusive quantities. In the region where collider data exist, below $E_{\text{CR}} \approx 10^{17}$ eV, all MC models show a similar energy dependence consistent with the experimental results. Above 10^{17} eV, increasingly bigger differences appear, with PYTHIA 6 having higher $\langle p_T \rangle$ and smaller inelasticity than the rest of models, but being in the “average” region with regards to charged particle multiplicity and inelastic cross section values. The largest model differences show up in the prediction of the energy dependence of the inelasticity, where PYTHIA 6 features an almost flat behavior with proton energy, to be compared to a 25–30% increase observed for EPOS-LHC, QGSJET-II-04, and QGSJET 01 between 10^{14} eV and 10^{20} eV. Since $\langle X_{\text{max}} \rangle$ and its average fluctuation $\sigma_{X_{\text{max}}}$ are mostly driven by the pp inelastic cross section and inelasticity, the EAS simulated with PYTHIA 6 feature larger penetration in the atmosphere than those from the rest of event generators, as discussed next.

B. Generic features of proton-induced EAS

Figure 2 shows the average position of the shower maximum in the atmosphere $\langle X_{\text{max}} \rangle$ (left) and the width of the fluctuations of the shower maximum position $\sigma_{X_{\text{max}}}$ (right) as a function of the incident cosmic-ray proton energy for inclined showers ($\theta = 60^\circ$). As expected for showers generated with our “Jupiter-like” hydrogen atmosphere, the elongation rate is higher than for standard air showers [44], leading to a high value of $\langle X_{\text{max}} \rangle$ at high energy. Indeed the slope of the energy evolution of the inelastic cross section is about twice larger in the case of p-p compared to p-Air interactions [44]. The cross section itself is about three times smaller in p-p than in p-Air, leading to larger values of $\sigma_{X_{\text{max}}}$ at low energy. Although all MCs predict relatively similar values for both quantities, PYTHIA 6 (all tunes, indistinguishably) features the largest $\langle X_{\text{max}} \rangle$ values, i.e., the largest penetration in the atmosphere, and the lowest $\sigma_{X_{\text{max}}}$, i.e., the smallest fluctuations in the altitude where the shower maximum appears.

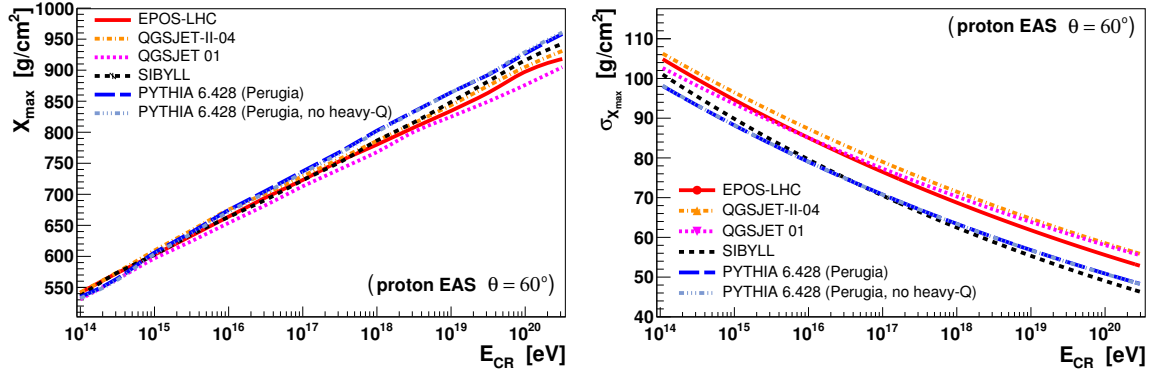


FIG. 2: Mean slant depth of the shower maximum $\langle X_{\text{max}} \rangle$ (left) and width of its associated fluctuations $\sigma_{X_{\text{max}}}$ (right) for inclined ($\theta = 60^\circ$) proton-induced showers as a function of the incoming cosmic-ray energy (E_{CR}), predicted by the six MC event generators considered here.

In general, the model that gives closest (resp. farthest) results to PYTHIA 6 is SIBYLL 2.1 (resp. QGSJET 01), whereas EPOS-LHC shows an intermediate behavior among all models. At $E_{\text{CR}} \approx 10^{20}$ eV, PYTHIA 6 predicts a shower maximum at a depth that is ~ 80 (50) g cm^{-2} larger than that of QGSJET 01 (EPOS-LHC). More surprising are the increasing differences among RFT model predictions. The difference in $\langle X_{\text{max}} \rangle$ between EPOS-LHC and QGSJET-II-04 is reduced from about 20 g cm^{-2} for p-Air, to less than 10 g cm^{-2} for p-p, the QGSJET-II-04 values being larger than those from EPOS-LHC, a result reversed compared to that found for air showers [44]. This is a clear sign that nuclear effects play a non-negligible role, and are an important source of uncertainties, in the hadronic MC simulations. In terms of the fluctuations of the altitude of the maximum shower, PYTHIA 6 and SIBYLL 2.1 share very similar behavior with about 5–10 g cm^{-2} smaller fluctuations than the rest of models, with QGSJET-II-04 giving the largest values of $\sigma_{X_{\text{max}}}$. The coincident results of PYTHIA 6 and SIBYLL 2.1 are largely accidental because, as can be understood from Fig. 1, they are due to a similar net cancellation of many different underlying physical effects. Whereas the larger penetration of PYTHIA 6 showers is mostly due to a low pp inelasticity (Fig. 1, bottom right), in the SIBYLL 2.1 case this is due to the

small number of particles produced per pp collision (Fig. 1, top right). The results of Fig. 2 also show that switching-off heavy-quark production in PYTHIA 6 has no effect on such inclusive EAS properties.

C. Electromagnetic properties of proton-induced EAS

About two-thirds of the secondary particles produced in a hadronic collision are pions, with similar amounts of π^0 , π^+ and π^- created. The neutral pions decay almost immediately into two photons which, at their turn, generate e^+e^- pairs which then lose further energy through new γ radiation, thereby generating an electromagnetic cascade in the atmosphere. Being well-known QED processes (bremsstrahlung, pair production, and ionization), the e.m. part of the shower is well under control from a theoretical point of view. Figure 3 (left) shows the total number of electrons and positrons at the shower maximum for inclined showers ($\theta = 60^\circ$) as a function of cosmic-ray proton energy E_{CR} , for all MCs considered in this work. The distribution is normalized by the E_{CR} value in order to display features that are otherwise difficult to discern in a steeply-falling spectrum. All models predict a similar amount of e^\pm at shower maximum (within $\sim 10\%$), with PYTHIA 6 and QGSJET 01 being in-between SIBYLL 2.1 and EPOS-LHC (that feature, respectively, the largest and lowest $N_{e^\pm\text{max}}$ values). All models show a moderate increase of $N_{e^\pm\text{max}}$ up to $E_{\text{CR}} \approx 10^{18}$ eV, followed by a decrease beyond that energy. This is due to the fact that above this energy, π^0 start to collide with the target nuclei, rather than decay, giving less energy to the e.m. component of the shower.

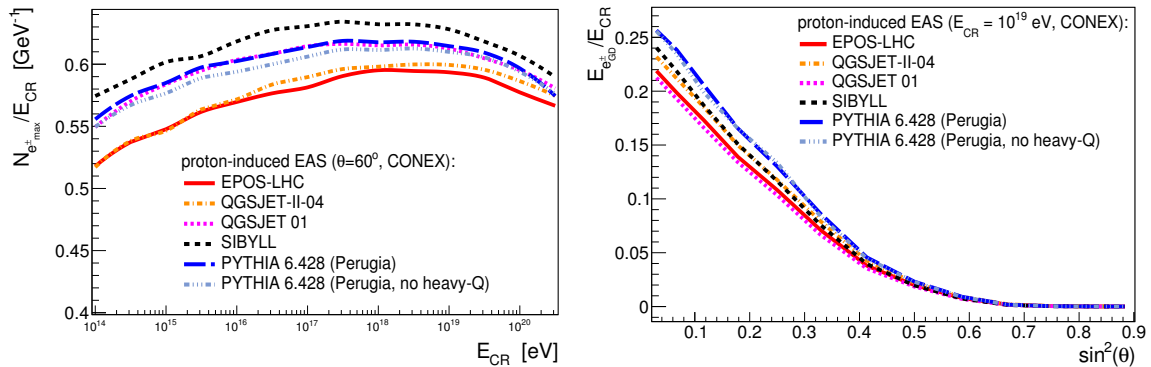


FIG. 3: Number of electrons and positrons at the shower maximum (normalized by the cosmic-ray energy E_{CR}) as a function of E_{CR} for inclined proton-induced showers with $\theta = 60^\circ$ (left), and fraction of shower e.m. energy at sea-level as a function of the (squared-sine) zenith angle for incoming protons with $E_{\text{CR}} = 10^{19}$ eV (right), predicted by the six MC event generators considered in this work.

The zenith-angle dependence of the fraction of UHECR energy carried by e^\pm and γ at ground for proton-induced EAS with $E_{\text{CR}} = 10^{19}$ eV is shown in Fig. 3 (right). Inclined showers ($\theta = 60^\circ$) are on the right of the plot ($\sin^2\theta = 0.75$), whereas the leftmost values are for fully vertical EAS ($\sin^2\theta = 0$). One sees that the amount of electron energy at ground is $\sim 25\%$ for vertical showers, decreasing to zero with decreasing CR incident angle in the atmosphere. The more vertical the shower is, the less comparatively absorbed its e.m. component is, and the closer the ground is to $\langle X_{\text{max}} \rangle$. Thus, here again, PYTHIA 6 features more e.m. ground energy than the rest of the models for more vertical showers, simply due to its predicted comparatively larger EAS penetration. We note also that switching-off heavy-quark production in PYTHIA 6 has no significant effect on the electromagnetic EAS properties.

D. Hadronic properties of proton-induced EAS

At variance with the electromagnetic properties of the proton-induced showers, that are very similar among MC models as shown in the previous section, larger differences appear in the hadronic properties of the EAS predicted by the different event generators. Figure 4 (left) shows the total number of hadrons produced at shower maximum (left) as a function of cosmic-ray proton energy E_{CR} for inclined showers ($\theta = 60^\circ$) normalized by the E_{CR} value. (Figure 4 (right) shows the UHECR energy fraction carried by hadrons at ground for proton-induced EAS with $E_{\text{CR}} = 10^{19}$ eV as a function of the (squared-sine of the) zenith angle of the incoming cosmic ray (right) for all MCs considered in this work. It is interesting to notice that at variance with the increasing number of e^\pm with E_{CR} (Fig. 3 left), less and less hadrons are present at shower maximum for larger primary energies. This is so because the maximum of the EAS is reached after an increasing number of

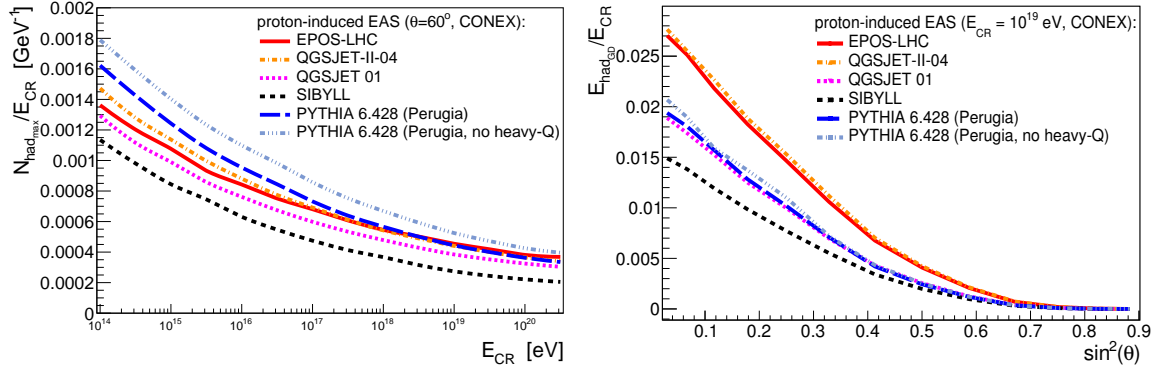


FIG. 4: Number of hadrons at shower maximum, normalized by the total CR energy, for inclined proton-induced showers ($\theta = 60^\circ$) as a function of cosmic-ray energy E_{CR} (left) and fraction of the total energy of the shower carried by hadrons at sea-level for proton-induced EAS with $E_{\text{CR}} \approx 10^{19}$ eV as a function of the (squared-sine) zenith angle of the incoming cosmic ray (right), predicted by the six MC event generators considered here.

hadronic generations, where about 20–30% of the energy is given to the e.m. component via π^0 decay. In terms of the number of hadrons at shower maximum (left panel), PYTHIA 6 (in particular *without* charm and bottom production) predicts the largest values among MC generators, very similar to those expected by EPOS-LHC and QGSJET-II-04; whereas SIBYLL 2.1 and QGSJET 01 generate about 50% less. However, EPOS-LHC and QGSJET-II-04 ground-level showers have about 35% or 80% more hadron energy fraction than predicted by PYTHIA 6, SIBYLL 2.1, or QGSJET 01 (Fig. 4, right). That EAS simulated with SIBYLL 2.1 feature less hadrons is not unexpected at first sight, given the lower particle multiplicity per pp collision predicted by this model, but this is in contradiction with the largest value predicted by QGSJET 01 (Fig. 1, top right). The underlying mechanism responsible of such differences requires further investigation.

As found for the e.m. component, the fraction of shower energy carried by hadrons at ground is increasingly reduced, by absorption in the atmosphere, for decreasing angles of incidence. The EAS simulated with EPOS-LHC and QGSJET-II-04 feature higher hadron energy fractions at ground for all zenith angles, and PYTHIA 6 (with and without heavy-quark production) have a very similar fraction and inclination-dependence as found with QGSJET 01, whereas SIBYLL 2.1 is clearly below the rest of the models. This is better seen in Fig. 5

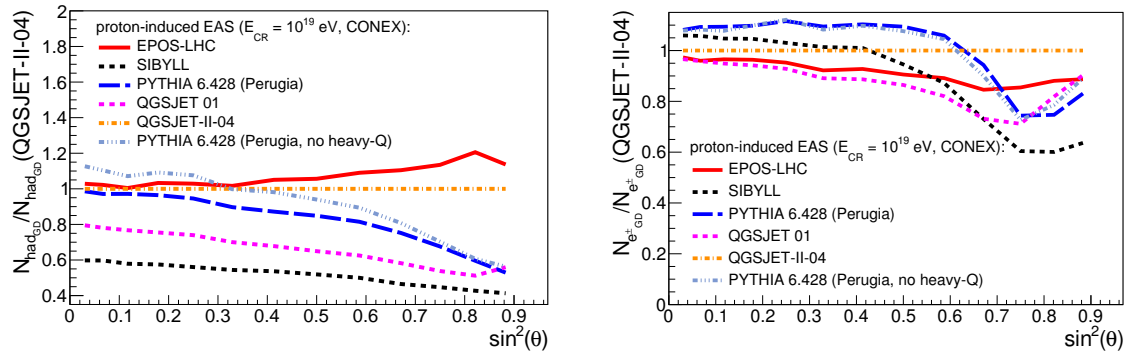


FIG. 5: Zenith-angle dependence of the number of hadrons (left) and electrons (right) at sea-level for proton-induced EAS of $E_{\text{CR}} = 10^{19}$ eV, predicted by the six MC event generators considered in this work *over* the QGSJET-II-04 prediction.

(left), that compares the results of all the models with respect to the QGSJET-II-04 prediction. The fast drop of the hadron production with zenith-angle seen for PYTHIA 6 showers, indicates that the hadronic component is absorbed relatively faster by the atmosphere for this MC generator than for the other models. The same phenomenon is observed for electrons in Fig. 5 (right), except for very inclined showers where an increase, related to the muonic component, is observed. Indeed, in that case, the electrons are coming from the decay of muons that are less attenuated by the atmosphere as shown in the next section.

E. Muonic properties of proton-induced EAS

Whereas UHECRs detected straight from above the observatories have EAS dominated by their e.m. component, photons and electrons are increasingly absorbed by the atmosphere in more inclined showers. At the same time, the larger the column of air in non-vertical showers, the larger the number of charged hadrons that decay into muons. Thus, ultimately, the muon component dominates the shower composition for angles of arrival above $\theta \approx 45\text{--}50^\circ$. The study of the muon properties (number density, energy, distance from the shower axis) at ground-level in inclined EAS provides thereby important insights on the hadronic development of the shower. Figure 6 shows the number of muons at shower maximum (normalized by $E_{\text{CR}}^{0.9}$ to flatten out the distribution according to the generalized Heitler model [41]) for inclined showers ($\theta = 60^\circ$) as a function of cosmic-ray energy for PYTHIA 6 and the RFT-based MC generators (left), and for the seven different PYTHIA 6 tunes (right). The EAS generated with PYTHIA 6 produce about the same number of muons as those

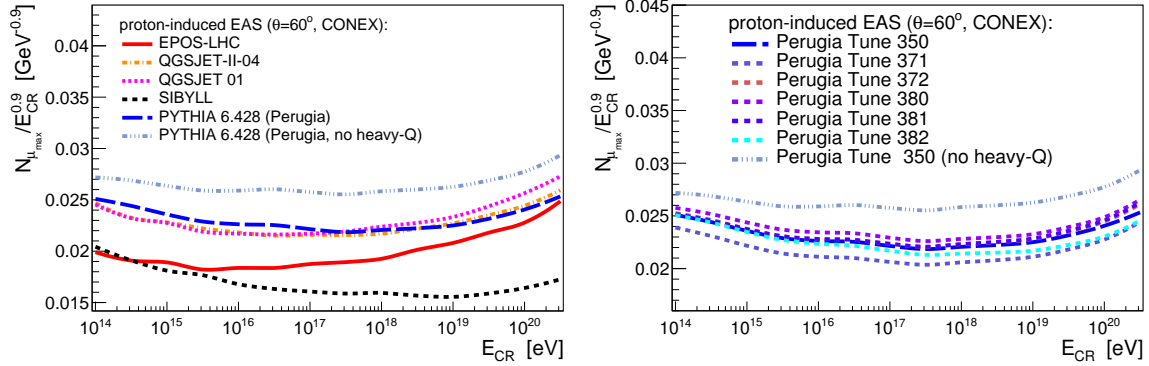


FIG. 6: Number of muons (normalized by $E_{\text{CR}}^{0.9}$) at shower maximum for inclined proton-induced showers ($\theta = 60^\circ$) as a function of cosmic-ray energy, predicted by the six MC event generators (left), and for the seven PYTHIA 6 tunes (right) considered here.

from QGSJET-II-04 and QGSJET 01, and 25–50% more than SIBYLL 2.1. Interestingly, whereas the different PYTHIA 6 tunes yield consistent number of muons within $\pm 5\%$, running PYTHIA 6 without heavy-quarks production generates $\sim 15\%$ more muons at shower maximum than all other MCs. This result indicates, first, that the main source of muons in PYTHIA 6 is clearly the decays of light-quark mesons (charged pions and kaons), and that heavy-quark production accounts for a negligible fraction of the total inclusive muons. Second, switching-off charm and bottom production seems to leave more room for π^\pm and K^\pm production, and thereby for an increased muon density in the showers. The main conclusion of this study is that, at least for a hydrogen atmosphere, there are “non-exotic” ways to increase by at least 15% the muon density in the showers at ground. A similar conclusion has been reached with the latest version (2.3c) of SIBYLL [45], that includes the production of heavy flavors and leads to a number of muons comparable to that of EPOS and QGSJET-II-04 [44]. Unfortunately, this latter MC generator was too recent to be tested with the modified atmosphere used in the current study. In any case, one must be reminded that for real UHECR collisions on air, at variance with the result found for proton-hydrogen collisions, EPOS-LHC produces more μ^\pm than

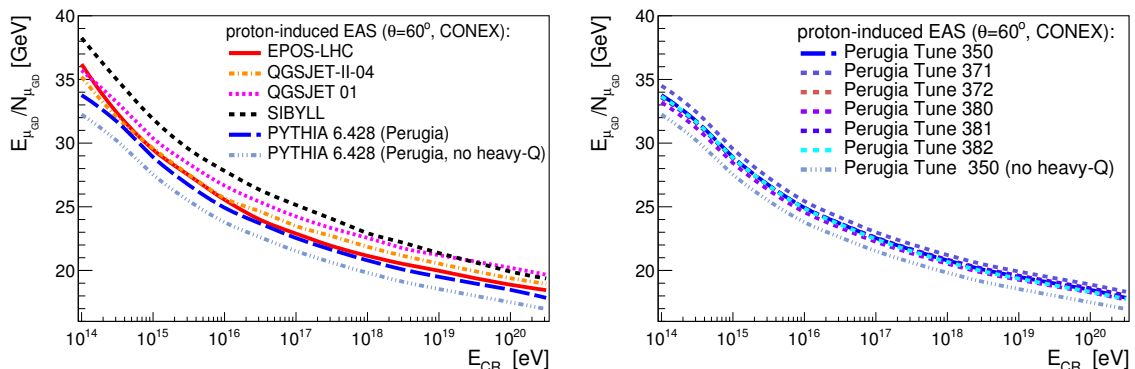


FIG. 7: Mean energy of muons at sea-level for inclined proton-induced showers ($\theta = 60^\circ$) as a function of cosmic-ray energy (E_{CR}) predicted by the six MC event generators (left), and for the seven PYTHIA 6 tunes (right) considered here.

QGSJET-II-04 with a similar E_{CR} -dependence [44], while in Fig. 6 (left) the slope of N_μ versus E_{CR} predicted by EPOS-LHC is very different to that of all other models. Therefore, nuclear effects, absent in our current setup, definitely also play a role in the final inclusive production of muons measured in the data.

The average energy of the muons reaching sea-level for inclined showers ($\theta = 60^\circ$) is shown in Fig. 7 as a function of cosmic-ray energy for PYTHIA 6 and the RFT-based MC generators (left), and for the seven different PYTHIA 6 tunes (right). For such an observable, the features of the PYTHIA 6 proton-induced showers are below the rest of the models: PYTHIA 6 predicts $\sim 5\%$ less energy per muon at ground than QGSJET-II-04 and up to $\sim 10\%$ less than QGSJET 01 or SIBYLL 2.1, and only slightly below EPOS-LHC. The right panel of Fig. 7 indicates small differences among PYTHIA 6 tunes, although without heavy-quarks, PYTHIA produces more than 5% less energetic muons. This is easily understood by the fact that high-energy μ^\pm coming from heavy-flavor meson decays are replaced by many more low energy muons produced after a long chain of hadronic interactions.

The energy (left) and zenith-angle (right) dependence of the fraction of total energy carried by muons on ground for cosmic rays with $E_{\text{CR}} = 10^{19}$ eV are shown in Fig. 8. The fraction of UHECR energy carried by muons is much less dependent on zenith angle than for e^\pm and charged hadrons (right panels of Figs. 3 and 4). A similar hierarchy of MC generators is found for the E_{CR} - (left) and for the θ - (right) dependent results. The QGSJET-II-04 and QGSJET 01 simulations feature the largest fraction of energy carried by muons at sea-level, followed by PYTHIA 6 without heavy-quark production, EPOS-LHC, PYTHIA 6 (tune 350), and SIBYLL 2.1. A slightly smaller attenuation length (steeper slope) is observed in the zenith-angle dependence of PYTHIA 6, irrespectively of heavy flavor production, compared to all other models. This is consistent with the lower mean energy of the muons observed in Fig. 7, and with the attenuation of the hadron component shown in Fig. 5.

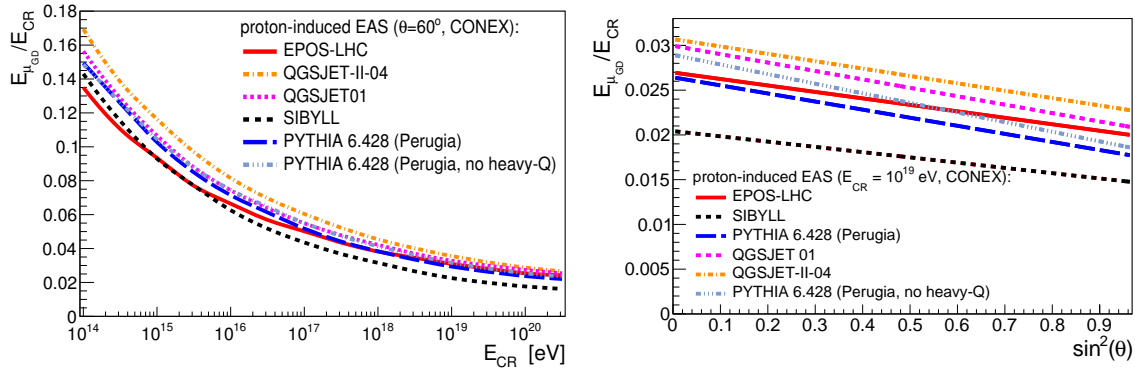


FIG. 8: Fraction of the CR energy carried by muons at sea-level for inclined proton-induced showers ($\theta = 60^\circ$) as a function of cosmic-ray energy (E_{CR}) (left), and as a function of the (squared-sine) zenith angle of the incoming cosmic ray with $E_{\text{CR}} \approx 10^{19}$ eV (right), predicted by the six MC event generators considered in this work.

To further study the muon properties of the generated EAS, Fig. 9 (left) shows the zenith-angle dependence (left) and the radial (distance to the shower core) dependence (right) of the number of muons at sea-level predicted by the different MC simulations *over* the QGSJET-II-04 prediction (which is used as a reference here and features the largest muon density among all RFT-models), for proton-induced EAS of $E_{\text{CR}} = 10^{19}$ eV. Because of their lower average energy, the muons produced by PYTHIA 6 and QGSJET 01 are absorbed by the atmosphere faster than for the other models. Interestingly, Fig. 9 (right) indicates that PYTHIA 6 features in general less muons than other MCs closer to the core shower (40–200 m) but predicts more muons for transverse distances larger than 600-m from the shower axis. The latter result is even more dramatic for PYTHIA 6 without heavy-quark production, which predicts up to 25% more muons than QGSJET-II-04 for very inclined showers. The higher density of muons at large radial distances from the EAS core predicted by PYTHIA 6 is likely to be connected to the highest transverse momenta of the produced charged hadrons (that eventually decay into muons) in this pQCD-based Monte Carlo, as can be seen in the energy evolution of $\langle p_T \rangle$ plotted in Fig. 1 (bottom left). Minijets, fragmenting into high- p_T hadrons, are produced more copiously via multiparton interactions in PYTHIA 6 than in the rest of the MC event generators. A possible way to test if such a mechanism is responsible for the larger number of muons at large transverse distances from the EAS axis, would be to modify the RFT-based models so that their fixed soft-hard Q_0 cutoff (which controls the amount of pQCD minijets produced at a given \sqrt{s}) is changed to a power-law running behavior as implemented in PYTHIA 6.

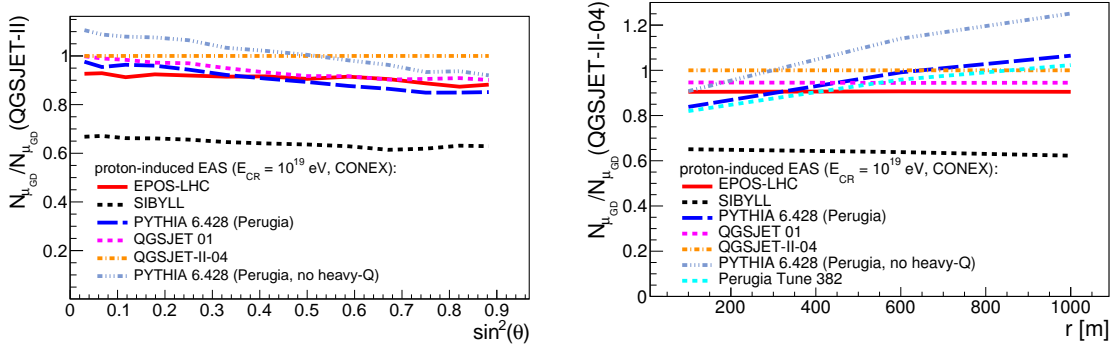


FIG. 9: Zenith-angle (left) and radial (distance to the shower core) (right) dependence of the number of muons at sea-level for proton-induced EAS of $E_{\text{CR}} = 10^{19}$ eV predicted by the six MC models considered here *over* the QGSJET-II-04 prediction.

IV. SUMMARY AND CONCLUSIONS

A detailed study of the properties of extended air showers (EAS) generated by cosmic-ray protons with energies $E_{\text{CR}} = 10^{14}$ – 10^{20} eV has been carried out with a fast CONEX simulation of a hydrogen atmosphere with the same density as air. The use of an atmosphere with “Jupiter-like” composition allows one to interface the PYTHIA 6 Monte Carlo (MC) event generator, commonly used in collider physics and tuned to reproduce the LHC proton-proton (pp) data, and compare its results to those predicted by hadronic MC generators typically used in cosmic-ray studies (EPOS-LHC, QGSJET-II-04, QGSJET 01, and SIBYLL). At variance with the latter hadronic models, based on Gribov’s Reggeon Field Theory (RFT), PYTHIA 6 contains factorized hard perturbative processes producing energetic QCD jets as well as charm and bottom quarks, that could potentially explain recent data–theory divergences, in particular, regarding the characteristics of the muons produced in EAS.

We have first studied the overall properties of pp collisions (inelastic cross section, charged-particle multiplicity, mean transverse momentum, and inelasticity) as a function of cosmic-ray energy, and found that all models reproduce the existing data up to equivalent energies of $E_{\text{CR}} \approx 10^{17}$ eV. Beyond that energy, models start to deviate in their predictions up to $E_{\text{CR}} \approx 10^{20}$ eV, with PYTHIA 6 producing increasingly larger transverse momenta particles, and having overall lower pp inelasticity than the rest of approaches. We have then compared the properties of the generated proton-induced showers for key EAS variables such as the mean altitude of the shower maximum $\langle X_{\text{max}} \rangle$ and the width of its associated fluctuations $\sigma_{X_{\text{max}}}$. Detailed characteristics of the electromagnetic, charged-hadronic, and muonic components of the EAS at the shower maximum and at sea-level have been studied as a function of the primary cosmic-ray energy, zenith-angle, and transverse distance from the shower axis.

The first generic conclusion reached is that, in general, the values and the E_{CR} -evolution of $\langle X_{\text{max}} \rangle$ and $\sigma_{X_{\text{max}}}$, as well as of the density and energy of e^{\pm} and charged-hadrons at sea-level, are quite similar in PYTHIA 6 and the standard cosmic-ray hadronic models. The second generic result is that changes in the PYTHIA 6 parameter settings (using different “tunes” of the semi-hard scattering and hadronization dynamics) result in very similar EAS properties, except when switching-off completely charm and bottom production, which leads to increased charged hadron and muon production, in particular at large transverse distances from the shower axis. The latter observation seems to indicate that heavy-quark production (decaying into hard muons) is *not* the physical mechanism responsible of the overall increased μ^{\pm} production observed in the data in comparison to the model predictions.

Looking into more detail, the PYTHIA 6 showers feature deeper penetration in the atmosphere (i.e., larger shower maximum position) and smaller $\sigma_{X_{\text{max}}}$ fluctuations, likely due to a reduced p-p inelasticity, compared to the other MC event generators (and similar to those predicted by SIBYLL, although for very different underlying physical reasons). The characteristics of the electromagnetic component of proton-induced PYTHIA 6 EAS are found in-between those of other MC generators. The PYTHIA 6 hadron shower density at shower maximum is similar to that found with EPOS-LHC and QGSJET-II-04, whereas the corresponding fraction of shower energy carried by hadrons at sea-level is smaller than the one predicted by the latter models

and more similar to SIBYLL or QGSJET 01.

The properties of the muon component of the proton-induced EAS in PYTHIA 6 are significantly different than those predicted by the RFT-based hadronic models. First, in general PYTHIA 6 predicts a total muon density and energy at sea-level in between that of other MCs (more than EPOS-LHC but a bit less than QGSJET-II-04). However, switching-off charm and bottom production seems to leave more room for charged pion and kaon production, and thereby for a 15% increased muon density in the showers. This result points out, first, that the main sources of muons in PYTHIA 6 are the decays of light-quark mesons (charged pions and kaons), and that heavy-quark production accounts for a negligible fraction of the inclusive muons. Secondly, this proves that, at least for a hydrogen atmosphere, there are “non-exotic” ways to increase by at least 15% the muon density in the shower at ground. However, one must be reminded that for real UHECR collisions on air, at variance with the results found in our proton-hydrogen collision setup, EPOS-LHC produces more μ^\pm than QGSJET-II-04. Therefore, nuclear effects, that are absent in our current setup, definitely also play a role in the final production of muons observed in the data [44].

The most clear-cut result is that PYTHIA 6 (with or without heavy-quark production) features increasingly harder muon lateral distributions compared to the rest of models. PYTHIA 6 showers feature a bit less muons close to the core (40–200 m radial distance), but 10–30% more at 600-m and at 1-km from the shower axis. The higher density of muons at large radial distances predicted by PYTHIA 6 is likely to be connected to the highest transverse momenta of the produced charged hadrons in this model. The underlying physical reason being that pQCD minijets, fragmenting into high- p_T hadrons and eventually decaying into hard muons, are produced more copiously via multiparton interactions in PYTHIA 6 than in the rest of the MC event generators.

In summary, this is the first time, to our knowledge, that the PYTHIA event generator has been used to analyze ultrahigh-energy cosmic-rays showers. Our study indicates that retuning the production of multiple (hard) minijets in the standard cosmic-rays MC generators, combined with improved nuclear effects, will have a bigger impact on the muonic EAS properties, and on the potential resolution of several muon “anomalies” observed in UHECR showers, than incorporating the generation of charm and bottom quarks into the RFT-based models. The present work provides novel insights into the microscopic dynamics of hadronic collisions that are relevant for the understanding of the energy and identity of the highest-energy cosmic-rays in the universe.

Acknowledgments

We are grateful to Awadallah Mekki for help in preliminary studies of this topic.

Bibliography

-
- [1] S. Mollerach and E. Roulet, Prog. Part. Nucl. Phys. **98** (2018) 85 [arXiv:1710.11155 [astro-ph.HE]].
 - [2] B. R. Dawson, M. Fukushima and P. Sokolsky, PTEP **2017** (2017) 12A101 [arXiv:1703.07897 [astro-ph.HE]].
 - [3] A. Aab *et al.* [Pierre Auger Collaboration], Nucl. Instrum. Meth. A **798** (2015) 172
 - [4] T. Abu-Zayyad *et al.* [Telescope Array Collaboration], Astrophys. J. **768** (2013) L1
 - [5] D. Heck, G. Schatz, T. houw, J. Knapp and J. N. Capdevielle, FZKA-6019 Report (1998)
 - [6] K. Werner, F. M. Liu and T. Pierog, Phys. Rev. C **74** (2006) 044902
 - [7] T. Pierog, I. Karpenko, J. M. Katzy, E. Yatsenko and K. Werner, Phys. Rev. C **92** (2015) 034906
 - [8] N. N. Kalmykov and S. S. Ostapchenko, Phys. Atom. Nucl. **56** (1993) 346 [Yad. Fiz. **56N3** (1993) 105]
 - [9] N. N. Kalmykov, S. S. Ostapchenko and A. I. Pavlov, Nucl. Phys. Proc. Suppl. **52** (1997) 17
 - [10] S. Ostapchenko, Phys. Rev. D **83** (2011) 014018
 - [11] E. J. Ahn, R. Engel, T. K. Gaisser, P. Lipari and T. Stanev, Phys. Rev. D **80** (2009) 094003
 - [12] W. R. Nelson, H. Hirayama and D. W. O. Rogers, SLAC-0265, SLAC-265, SLAC-R-0265, SLAC-R-265
 - [13] V. N. Gribov, Sov. Phys. JETP **26** (1968) 414 [Zh. Eksp. Teor. Fiz. **53** (1967) 654]
 - [14] D. d’Enterria, R. Engel, T. Pierog, S. Ostapchenko and K. Werner, Astropart. Phys. **35** (2011) 98
 - [15] A. Aab *et al.* [Pierre Auger Collaboration], Phys. Rev. D **90** (2014) 122005
 - [16] R. U. Abbasi *et al.*, Astropart. Phys. **64** (2015) 49
 - [17] S. Ostapchenko, Phys. Rev. D **89** (2014) 074009

- [18] T. Pierog, EPJ Web Conf. **99** (2015) 09002.
- [19] S. Ostapchenko, Proceeds. XXV European Cosmic Ray Symposium (2016), arXiv:1612.09461 [astro-ph.HE]
- [20] A. Aab *et al.* [Pierre Auger Collaboration], Phys. Rev. D **91** (2015) 032003; [Erratum: *ibid.* **91** (2015) 059901]
- [21] A. Aab *et al.* [Pierre Auger Collaboration], Phys. Rev. Lett. **117** (2016) 192001
- [22] T. Abu-Zayyad *et al.* [HiRes and MIA Collaborations], Phys. Rev. Lett. **84** (2000) 4276
- [23] F. Riehn, R. Engel, A. Fedynitch, T. K. Gaisser and T. Stanev, EPJ Web Conf. **99** (2015) 12001
- [24] T. Pierog and K. Werner, Phys. Rev. Lett. **101** (2008) 171101
- [25] J. Allen and G. Farrar, arXiv:1307.7131 [astro-ph.HE]
- [26] R. Aloisio, P. Blasi, I. De Mitri and S. Petrera, in R. Aloisio, E. Coccia, F. Vissani (eds.) “Multiple Messengers and Challenges in Astroparticle Physics”. Springer, Cham; arXiv:1707.06147 [astro-ph.HE].
- [27] T. Sjöstrand, S. Mrenna and P. Z. Skands, JHEP **0605** (2006) 026
- [28] P. Z. Skands, Phys. Rev. D **82** (2010) 074018
- [29] T. Bergmann *et al.*, Astropart. Phys. **26** (2007) 420
- [30] H. J. Drescher and G. R. Farrar, Phys. Rev. D **67** (2003) 116001
- [31] T. Pierog *et al.*, Proceeds. 32nd Intl. Cosmic Ray Conference (ICRC) 2011, doi:10.7529/ICRC2011/V02/1170
- [32] B. Andersson, G. Gustafson, G. Ingelman and T. Sjöstrand, Phys. Rept. **97** (1983) 31
- [33] G. A. Schuler and T. Sjöstrand, Phys. Rev. D **49** (1994) 2257
- [34] T. Sjöstrand and M. van Zijl, Phys. Rev. D **36** (1987) 2019
- [35] H. L. Lai *et al.* [CTEQ Collaboration], Eur. Phys. J. C **12** (2000) 375
- [36] J. Pumplin, D. R. Stump, J. Huston, H. L. Lai, P. M. Nadolsky and W. K. Tung, JHEP **0207** (2002) 012
- [37] T. Sjöstrand, S. Mrenna and P. Z. Skands, Comput. Phys. Commun. **178** (2008) 852 [arXiv:0710.3820 [hep-ph]]
- [38] D. d’Enterria and T. Pierog, JHEP **1608** (2016) 170 [arXiv:1604.08536 [hep-ph]]
- [39] V. A. Abramovsky, V. N. Gribov and O. V. Kancheli, Yad. Fiz. **18** (1973) 595 [Sov. J. Nucl. Phys. **18** (1974) 308]
- [40] M. Glück, E. Reya and A. Vogt, Eur. Phys. J. C **5** (1998) 461
- [41] J. Matthews, Astropart. Phys. **22** (2005) 387.
- [42] R. Ulrich, R. Engel and M. Unger, Phys. Rev. D **83** (2011) 054026
- [43] P. Abreu *et al.* [Pierre Auger Collaboration], Phys. Rev. Lett. **109** (2012) 062002
- [44] T. Pierog, EPJ Web Conf. **145** (2017) 18002
- [45] A. Fedynitch, F. Riehn, R. Engel, T. K. Gaisser and T. Stanev, arXiv:1806.04140 [hep-ph].